

Depth-of-Focus and its Association with the Spherical Aberration Sign. A Ray-Tracing Analysis

Ravi C. Bakaraju¹⁻³, Klaus Ehrmann¹⁻³, Eric B. Papas¹⁻³ and Arthur Ho¹⁻³

ABSTRACT

PURPOSE: To investigate the relationship between the sign of spherical aberration (SA) and the corresponding depth-of-focus (DoF) values around best focus, at three different spatial frequencies (SF). Additionally, to study the influence of the Stiles-Crawford effect (SCE) on DoF.

METHODS: We modeled schematic eyes having a range of SA values, C (4, 0), from -0.20 to 0.20 μm , at 6 mm pupil, in a ray-tracing software (Zemax). The through-focus optical performance was obtained via Modulation Transfer Function (MTF) calculations using thin paraxial lenses in-front of the model eye, from -2.00 to +2.00 D in 0.05D steps. Through-focus full-width (defocus) occurring at the half maximum of MTF value was considered as DoF, in diopters.

RESULTS: For the low-SF configuration, +SA and -SA results were close to being mirror symmetries of one another. However, for mid- and high- SF targets, in the SA range spanning from -0.15 to 0.15 μm , models of equal SA magnitude but opposite sign produced similar DoF measures, but those with SA more negative than -0.15 μm showed marginally higher DoF than their positive counterparts. The SCE improved DoF for low SF (10 cycles/mm), while for mid and higher SF (>30 cycles/mm) mixed results were observed.

CONCLUSIONS: As regards presbyopic-correction strategies that use deliberately induced aberrations to increase the depth of focus, the current study suggests that both positive and negative SA have equal potential. However, practical considerations will probably limit the useful DoF achievable through the utilization of SCE in presbyopes. for reference to a contemporary record detailing refractive history. (J Optom 2010;3:51-59 ©2010 Spanish Council of Optometry)

KEY WORDS: depth-of-focus; spherical aberration; eye model; Stiles-Crawford effect.

RESUMEN

OBJETIVO: Investigar, para tres frecuencias espaciales (FE) distintas, la relación entre el signo de la aberración esférica (AE) y la corres-

pondiente profundidad de foco (PdF) alrededor del mejor foco. Además, se estudiará cómo afecta el efecto Stiles-Crawford (ESC) a la PdF.

MÉTODOS: Hemos utilizado un modelo de ojo esquemático con distintos valores de aberración esférica (AE) (C (4, 0) comprendido entre 0.20 y 0.20 μm , para un diámetro de pupila de 6 mm) para investigar la relación que existe entre el signo de la AE y la correspondiente profundidad de foco (PdF) alrededor del mejor foco para tres frecuencias espaciales (FE) distintas. También se estudió la influencia del efecto Stiles-Crawford (ESC).

RESULTADOS: Para FE bajas, los resultados correspondientes a +AE y AE presentan simetría especular. Sin embargo, para FE medias y altas, y en el intervalo de AE comprendido entre 0.15 y 0.15 μm , modelos de igual AE (en módulo) pero distinto signo da lugar a valores de PdF similares, pero para valores de AE más negativos que 0.15 μm se obtuvieron PdF ligeramente más altas que para un valor positivo equivalente de AE. El ESC hace que aumente la PdF para FE bajas (10 ciclos/mm), mientras que para FE medias y altas (>30 ciclos/mm) se observan resultados variados.

CONCLUSIONES: En lo que respecta a las estrategias de corrección de la presbicia basadas en la inducción deliberada de aberraciones para aumentar la profundidad de foco, el presente estudio sugiere que valores positivos de la AE tienen el mismo potencial que los equivalentes negativos. Sin embargo, es probable que las consideraciones de tipo práctico limiten el rango de valores útiles de PdF que se pueden lograr mediante la utilización en presbiopes del ESC.

(J Optom 2010;3:51-59 ©2010 Consejo General de Colegios de Ópticos-Optometristas de España)

PALABRAS CLAVE: profundidad de foco; aberración esférica; modelo de ojo; efecto Stiles-Crawford.

INTRODUCTION

When the eye is in-focus, the retinal image plane is always optically conjugate with the object of regard. A certain range closer or farther away from the initial object position causes an imperceptible blurring of the retinal image. This is defined as the depth-of-field and is dioptrically analogous to the depth-of-focus (DoF) on the retina. Both the geometrical and the physical properties of an optical system can be used to predict these phenomena. The former method employs principles of paraxial optics, like controlled growth of spot sizes, while the latter accounts for diffraction and can be derived from the modulation transfer function (MTF) calculations. Since it is well agreed that the eye, though robust, is optically imperfect due to the presence of aberrations,¹ it seems more appropriate to derive these measures from the physical-optics standpoint.

The DoF of the human eye is not only a function of optical parameters such as pupil size and aberrations, but is also affected by retinal, neural and more complex psychophysical factors.²⁻⁴ Among these, the Stiles-Crawford effect (SCE) is one of the most important retinal factor. This is a consequen-

From ¹Institute for Eye Research, Sydney, Australia. ²Vision Co-operative Research Centre, Sydney, Australia. ³School of Optometry and Vision Science, UNSW, Sydney, Australia

Acknowledgements: This research was supported in the form of a University International Postgraduate Research Scholarship from the UNSW, Sydney, Australia and Top-up Scholarship from the Institute for Eye Research and Vision Cooperative Research Centre, Sydney, Australia to the first author (RCB). This study was carried while RCB was a recipient of the Contact Lens Society of Australia award (2008 & 2009) and William. C. Ezell fellowship from the American Optometric Foundation (2009). The authors extend a special thanks to the anonymous reviewer who provided insight into the plausible explanation for the marginal increase in depth-of-focus measures with negative spherical aberration condition in few conditions

Received: 19 July 2009

Revised: 17 October 2009

Accepted: 19 October 2009

Corresponding author: Ravi Chandra Bakaraju, 3049, RMB-NW, Gate 14, UNSW, Barker Street, Kensington, Sydney NSW 2033, Australia e-mail: r.bakaraju@ier.org.au

ce of the directional sensitivity of the foveal photoreceptors whereby they elicit a visual response more efficiently when the incoming pencil of light lies close to the optical axis (from centre of the pupil) rather than when it enters obliquely. This effect has often been used to explain why the DoF does not decrease as rapidly as predicted by the geometrical model when the pupil size increases. The underlying idea is that the reduced impact of marginal rays due to the SCE reduces the effective pupil size and, therefore, increases the DoF.

It is known that the MTF of an unaberrated eye shows greater sensitivity to defocus than an optical system with aberrations. Although, these aberrations compromise the MTF at best-focus, they increase its relative measure with defocus and, therefore, result in a higher DoF.⁵ Thus, the DoF of an aberrated system is always higher than the equivalent unaberrated, or diffraction-limited, system. Additionally, monochromatic aberrations such as spherical aberration (SA) introduce blur to the visual system, rendering it less susceptible to the influence of chromatic aberration.^{6,7} These are examples of how aberrations can make a positive contribution to the optics of the eye. Clinically, this principle is utilized as a passive approach to correcting presbyopia with multifocal contact and intra-ocular lenses.

To understand how DoF might be optimally utilized in a corrective device, it is of value to consider how it is affected by changes in various aspects of the ocular system. For instance, its decrease with increasing pupil size, especially in aberration-free systems is a well-known fact. Moreover, studies have shown that the DoF is inversely related to spatial frequency.^{8,9} While in ideal eyes this effect is evident across the full range of relevant spatial frequencies, in real eyes it is only of importance up to about 8 cycles/degree; above that the DoF becomes virtually constant.¹⁰ Nevertheless, lower spatial-frequency targets produce retinal contrast profiles that are more tolerant to defocus.¹¹

The contribution of spherical aberration (SA) to the enhancement of presbyopic vision and post-cataract (IOL) surgery has been a topic of interest and debate among the vision scientists in the recent past.^{5,7,10,12-17} Although most agree that the multifocal effect of low-level SA increases the eye's depth of focus and leads to pseudo-accommodation,^{5,7,8,10,13,17} there are a few others who also demonstrated an improvement in the subjects' spatial vision at the best-focus position without compromising the subjective tolerance to defocus, despite a complete correction of the ocular SA.^{12,15,16} These contradictory findings leave the clinicians and surgeons doubtful, whether or not to leave the patient with the residual amounts of SA for the benefit of DoF.

Adding further to the complexity, the exact association between the sign of SA and the effective DoF has also not been well comprehended. Some researchers proposed and proved that the inherent blur induced by positive SA would leave the patient less susceptible to the effects of defocus and chromatic aberrations.^{5,7,10,17} The patent issued to Somani and Yee¹⁸ claims that negative SA provides significantly larger DoF than a positive SA of the same magnitude, which would be sufficient to mitigate presbyopic symptoms. However, there has been no additional evidence supporting this posi-

tion. The accuracy of this proposal has considerable clinical ramifications as it could influence the design of multifocal corrective devices (e.g., IOLs), contact lenses and, potentially, presbyopic corneal ablations. This diversity of opinions amongst researchers and clinicians supports the need for further clarification. Accordingly, in the present work we sought to explore the influence of SA's sign on the optical DoF by using a ray tracing simulation. In addition, we also investigated the influence of the SCE, modeled as pupil apodization, on the spatial performance of centered optical systems.

METHODS

Modeling for Various Levels of Ocular Spherical Aberration (SA)

Eye models provide reasonably complete and realistic descriptions of the optical system of the eye. Among the various eye models proposed in the past, only a few are very similar to the average human eye in all respects, including both on- and off-axis aberrations.¹⁹ One of these is the Navarro-Escudero schematic eye model.²⁰ Considering this as baseline, we modeled eyes having different levels of spherical aberration (value of C (4, 0) ranging from -0.20 to 0.20 μm , for a 6 mm pupil diameter at a reference wavelength of 589 nm), which reflects the normative distribution of spherical aberration across the population.²¹ An important modification was introduced into the Navarro-Escudero model for the sake of brevity in the optimization procedure: the lenticular conic constants were slightly altered so as to yield a spherical-aberration-free baseline model. Later, into-the-eye ray tracing was carried out for each eye model using Zemax optical design software (Focus Software, Inc). In all the models the pupil plane was located immediately in front of the anterior crystalline lens surface. The entrance pupil, as seen from the air, was considered to be the aperture stop for the complete analyses.

When the model eye is highly aberrated and/ or entrance pupil is shifted or tilted, it is important to find rays at the object that correctly fill the aperture-stop surface for a given diameter. As all of our models were considerably aberrated, an in-built, iterative algorithm in the software called Ray-aiming was used for this purposed. The Ray-aiming algorithm was kept active in real, robust, cache mode. The "robust" mode adds an additional check, to make sure that if multiple ray paths to the same location on the stop surface exist, only the correct one is chosen, while the "cache" stores the coordinates so that new ray traces can take advantage of previous iterations.

A custom-written macro in the Zemax environment executed the ray tracing and optimization procedure. For the latter, a merit function was set-up with several weighted operands.

These included:

- 1) The specified amount of SA for the respective models: C (4,0), for a 6 mm pupil
- 2) An emmetropic 2nd-order refraction, with Mean Spherical Equivalent (MSE), Astigmatic terms (J180 and J45) zeroed
- 3) A minimum RMS spot radius

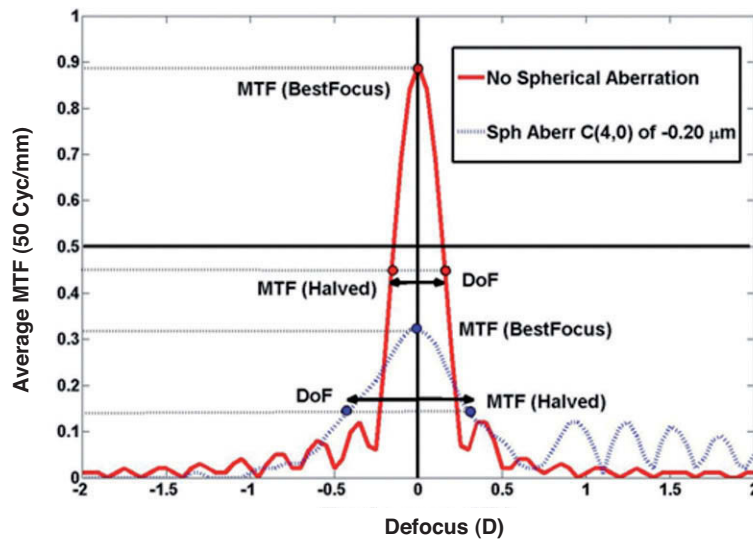


FIGURE 1

Through-focus MTF both for an aberrated and an unaberrated schematic eye model. Depth-of-focus (D) is defined as the defocus range for which the MTF stays above 50% of its maximum value. The red bold line represents the unaberrated system, while the blue dashed line represents a model with $-0.20 \mu\text{m}$ of spherical aberration (Zernike coefficient $C(4, 0)$).

All operands were given the same weighting, equal to one. The anterior corneal surface of each model was represented using the Zernike standard phase surface type (simulating a phase plate). This surface has a substrate shape identical to the standard surface, which supports spheres and conic sections, as well as the phase terms defined by the use of Zernike standard coefficients. These additional phase terms deviate and add optical path to the rays that go through the surface. Such models are very well suited to incorporate aberrations into the system.

In the current experiment, the $C(4,0)$ term of the Zernike standard phase surface expansion along with the vitreous chamber depth were defined as the variables for the damped, least-squares optimization method. A 512×512 ray grid density covering the complete entrance pupil was used for all the optical calculations. Since the ray tracing was performed assuming an on-axis object point, the chance of asymmetric aberrations (e.g., coma, trefoil) being included into the total magnitude of higher-order aberrations (HOA) was negligible. Moreover, as defocus was forced to be zero, the HOA magnitude could be completely attributable to SA.

Modeling Stiles-Crawford Effect (SCE)

Although the SCE is in reality a photoreceptor phenomenon, it was modeled by including an apodized pupil filter, whose density gradually increased from the center towards the edge. This was incorporated into the model by modifying the transmission function: instead of being a uniformly lit pupil it was set to be a Gaussian apodized pupil with a SCE factor²² of 0.12 mm^{-2} (this value is an estimate derived from psychophysically conducted measurements).

Modulation Transfer Function Calculations

The Optical Transfer Function (OTF) is an objective measure of the quality of any optical system. It describes the effect of aperture diffraction and optical aberrations on

the image of a sinusoidal distribution of light intensity as a function of the spatial frequency of this distribution.²³ This is a complex function, whose real part is termed the Modulation Transfer Function (MTF) and whose complex argument is called the Phase Transfer Function (PTF).

The Point Spread Function (PSF) and the wave aberration are related by means of an integral equation known as the Fourier transform. Let us consider the optical system of the eye, and let the pupil transmission function be $T(x,y)$ and its wavefront aberration at the exit pupil $W(x,y)$. The pupil function at the exit pupil plane without taking into account the Stiles-Crawford effect would be,

$$\text{Pupil Function (P)} = T(x,y) * e^{-\frac{2\pi i}{\lambda} W(x,y)}$$

$$\text{Point Spread Function (PSF)} = \text{FT}(P, * \text{conj}(P))$$

$$\text{Optical Transfer Function (OTF)} = \text{FT}(\text{PSF})$$

$$\text{Optical Transfer Function (OTF)} = \text{MTF} * e^{-i \cdot \text{PTF}}$$

In the above equations, 'FT' represents a two-dimensional Fourier transform and 'conj' denotes complex conjugate term. The term 'PTF' stands for Phase Transfer Function.

All these calculations were internally computed by Zemax, the Fast Fourier Transform (FT) based MTF in this software is always computed in pupil-space co-ordinates and assumes a reasonably uniform distribution of rays on the exit pupil plane (in cosine space, to be accurate). The horizontal response is taken as the response to a periodic target whose lines are oriented along the object space's X-axis, while the vertical response corresponds to a target whose lines are oriented along the Y-axis.

Depth-of-Focus Calculations

Both the vertical and the horizontal contributions of the MTF are the same when it comes to an on-axis optical

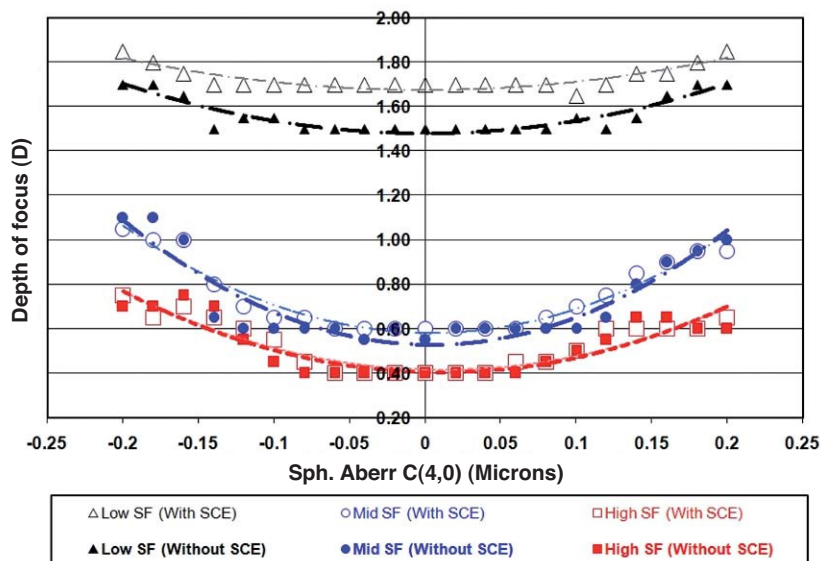


FIGURE 2

Depth-of-focus (D) measures as a function of spherical aberration (μm) for three different spatial frequencies, both with and without Stiles-Crawford effect (SCE). Depth-of-focus (D) is defined as the defocus range for which the MTF stays above 50% of its maximum value. Squares, circles and triangles in the figure represent high-, mid- and low- SF targets, respectively. Unfilled symbols represent calculations with SCE, while filled symbols indicate those calculations where the SCE has not been taken into account.

system. Hence, the MTF was described only by means of the vertical contributions of the modulus of the OTF. All the SA models were evaluated on-axis by calculating through-focus MTF performance at both sides of the best-focus, and executed using a custom-written macro. Through-focus full-width (defocus) occurring at the half maximum of MTF value was considered as DoF, in diopters. The DoF criterion is illustrated below, in *figure 1*.

In the Zemax software, this was obtained by placing just in front of the corneal surface a paraxial thin lens with variable power, which ranged from -2.00 to $+2.00$ D in steps of 0.05 D, to compute the through-focus MTF. A standard 512×512 sampling grid was used with a focus range of ± 2.00 D, at various testing frequencies and wavelengths.

Computational simulations were undertaken using different configurations; in particular:

- 3 Spatial Frequencies - 10 (Low), 30 (Mid) and 50 (High) cycles/mm
- 2 Accommodative states – Distance (Infinity) & near (33 cm)
- 2 Pupil diameters - 4 and 6 mm.
- With & Without SCE (for a 6-mm pupil)
- Monochromatic and Polychromatic light sources.

The DoF modeling was conducted for 2 independent pupil sizes for each of the different SA values, and for the near and far accommodative states. However, the SCE was included in the model only for the 6 mm pupil. To achieve the eye model parameters of the accommodated state, the optimization routine was recalled. For which, the unaccommodated state of the eye model was considered to be the starting point of this procedure. The lenticular radii of curvature, both anterior and posterior, along with their respective conic constants were subsequently named to be the operands

of the damped least-squares optimization procedure. For all the DoF calculations, the Zemax output files (containing the through-focus MTF yielded by the macro for the various configurations) were post-processed using custom-written Matlab® code.

Phase Transfer Function Calculations

The phase transfer function (PTF) accounts for the contributions of frequency and orientation of the phase to the OTF. Through-focus PTF's for all the SA values and configurations described above were evaluated using the 512×512 sampling grid and a large step size, again by means of the macro run in the Zemax environment. The range of dioptric focus change spanning from the best focus to the points where the first phase reversal occurs was considered to be the DoF definition from the phase perspective. Additionally, the number of phase reversals (180° phase shift) that occur for an arbitrary defocus value of ± 2.00 DS was also considered to be a useful relative metric.

RESULTS (DOF VERSUS SA)

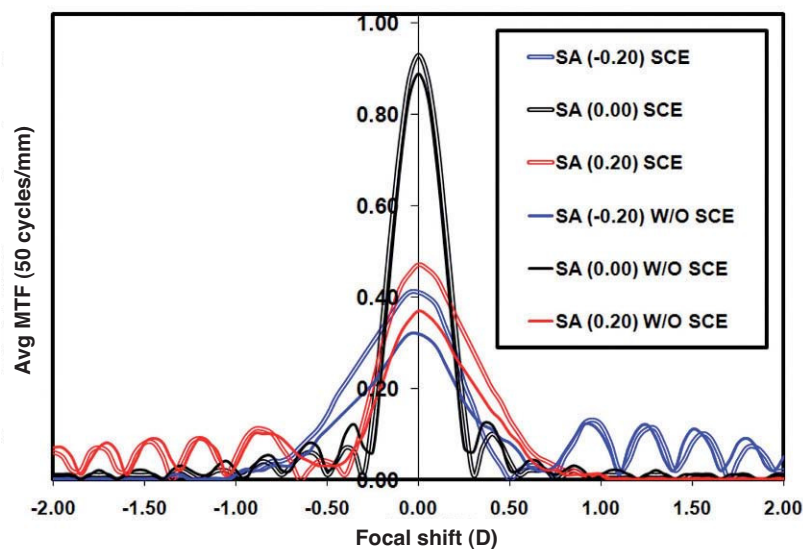
Distant Target, 6 mm Pupil, with & without SCE

The DoF data calculated for three different spatial frequencies (SF) as a function of SA, both with and without taking into account the SCE are illustrated in *figure 2*. As can be seen, the SCE increased the DoF for all the tested SF's. However, the impact of the SCE was consistent and predominant only for the lower SF targets and was found to be about 0.20 diopters across the different SA levels. When carefully observed, it can be noticed that, for mid- and high-SF targets, the SCE only produced a very slight increase in the DoF measures, ranging between 0.025 to 0.05 D. This was especially true for SA values within the -0.15 -to- 0.15

TABLE 1

Second-order polynomial fit and its resulting coefficient of determination (r^2) for each of the models under study: low/mid/high spatial frequency, with/without taking the Stiles Crawford Effect (SCE) into account

| Model | 2 nd Order Polynomial | r^2 |
|--------------------------------------|----------------------------------|-------|
| Low Spatial Frequency (With SCE) | $y = 3.543x^2 + 0.006x + 1.676$ | 0.78 |
| Low Spatial Frequency (Without SCE) | $y = 5.648x^2 + 0.003x + 1.479$ | 0.85 |
| Mid Spatial Frequency (With SCE) | $y = 11.65x^2 - 0.087x + 0.581$ | 0.94 |
| Mid Spatial Frequency (Without SCE) | $y = 16.34x^2 - 0.110x + 0.529$ | 0.87 |
| High Spatial Frequency (With SCE) | $y = 7.86x^2 - 0.175x + 0.418$ | 0.87 |
| High Spatial Frequency (Without SCE) | $y = 8.250x^2 - 0.168x + 0.405$ | 0.78 |

**FIGURE 3**

Through-focus MTF for three SA models, 0.00 μm , -0.20 μm and 0.20 μm , simulated at a spatial frequency of 50 cycles/mm, both with and without taking the Stiles-Crawford effect (SCE) into account. The double lines represent the calculations obtained with SCE, while the single solid lines represent measures without SCE. The black, blue and red colors represent no aberration condition, SA with -0.20 μm and SA with 0.20 μm respectively.

μm range. Outside this range, the DoF was barely affected by the SCE except for one or two cases, where signs of slight attenuation of about 0.10 D were evident, as can be seen in figure 2.

As predicted by theory, both positive and negative SA values resulted in an increase of the DoF. It can be seen that the +SA and the -SA results are close to showing mirrors symmetry, particularly for the low-SF configuration. Interestingly, for SA values ranging from -0.15 to 0.15 μm , models having equal SA magnitude but opposite sign produced similar levels of DoF, but those models with a negative SA below (i.e., higher in magnitude) -0.15 μm , showed a slightly higher DoF than their respective positive counterparts. The second-order polynomial fit and its corresponding coefficient of determinations (r^2) for each of the models tested (low/mid/high SF, with and without taking the SCE into account) are summarized in table 1.

Figure 3 demonstrates the trend of through-focus MTF for three of the SA models studied and also illustrates the impact

of the SCE on the MTF pattern. In all the aberration models, pupil apodization has slightly lifted the central peak of the MTF for the focused state. But with moderate levels of defocus, the plots obtained with and without SCE converged, until they became almost identical. Asymmetry in the MTF trend with the impact of defocus was only present in the aberrated models, negative as well as positive, ($\pm 0.20 \mu\text{m}$), and both with and without the inclusion of the SCE. This asymmetry manifests itself in two aspects, one in the peak width at half-maximum (PWHM) and the other in the form of unbalanced oscillations of the MTF with moderate to large levels of defocus.

PWHM for the -0.20 μm model were larger on the hyperopic side of the best-focus (i.e., the case where the paraxial image plane is in front of the retina), than on the myopic side. In the same model, the damped MTF oscillations ceased to zero at approximately 1.00 DS of hyperopia while they could be seen to persist up to 2.00 DS on the myopic side of the optimum-focus. Exactly the opposite happened for the +0.20 μm model.

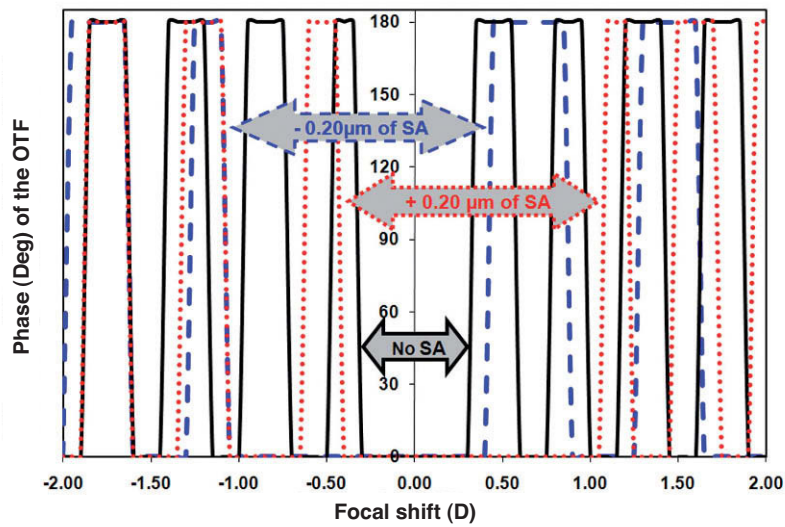


FIGURE 4
Through-focus Phase Transfer Function (PTF) for three SA values of the considered model, 0.00 μm , -0.20 μm and 0.20 μm , calculated for a spatial frequency of 50 cycles/mm, considering the Stiles-Crawford effect (SCE). The solid-black, dotted-red and dashed-blue lines represent the no aberration, +0.20 μm SA and -0.20 μm SA conditions, respectively.

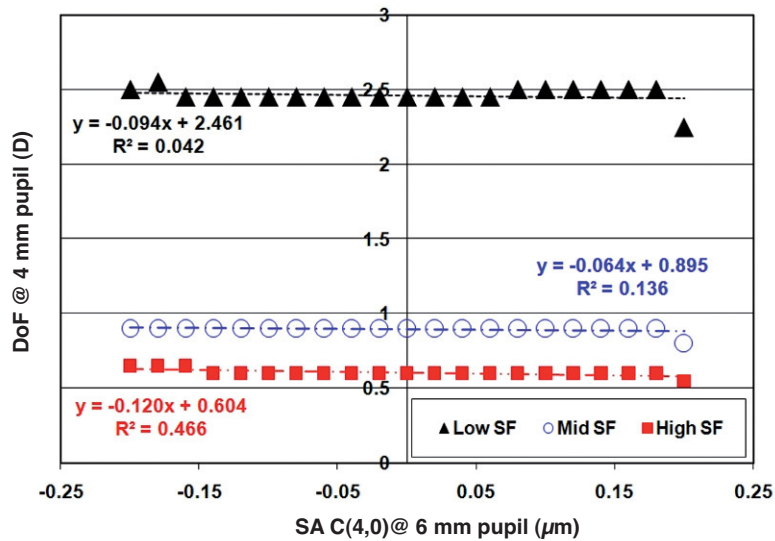


FIGURE 5
Depth-of-focus (D) for a 4 mm pupil diameter as a function of the spherical aberration coefficient C(4,0) (μm) computed for a 6 mm pupil, for three different spatial frequencies. For all the calculations the Stiles-Crawford effect was ignored. Results were identical for both far and near vergences tested.

Figure 4 shows the trends of through-focus PTF's for three representative examples chosen from the entire range of SA and SCE scenarios. The range of dioptric focus change from best-focus to the point where the first phase reversal occurs was relatively small in the unaberrated eye, compared to the aberrated cases. From the phase perspective, the DoF range among the +0.20 and -0.20 μm SA models was slightly asymmetric, with the -0.20 μm case showing slightly higher values. With ± 2.00 DS of induced defocus, for the unaberrated model there were about 8 phase reversals (180° phase shifts) on each side. Slightly fewer phase reversals occurred when aberrations of the same order of magnitude

as defocus were present. With positive SA, about 6 and 5 reversals occurred on the myopic and hyperopic sides respectively, while for negative SA the number of occurrences were 4 and 5.

All the through-focus MTF's in figure 3 show some oscillations. These are large and symmetrical for the unaberrated model, but smaller in number and asymmetrical for the aberrated cases. Oscillations on a modulated MTF could mean that a 180° phase shift occurs, and given that in this case they are well correlated with the PTF profiles described in figure 4, it appears that they truly represent phase shifts at the respective focal planes.

For Small Pupils and Accommodative Targets

Figure 5 shows a plot of the DoF for a 4 mm pupil diameter computed without SCE, as a function of the SA value computed for a 6 mm pupil. The three plots represent three different spatial frequencies. There were no noticeable differences in the DoF value over a range of SA. The resulting graphs were identical for both far and near vergences.

Monochromatic vs. Polychromatic Light

It has been shown that the inclusion of properly weighted chromatic aberrations into the modeling of optical and visual functions of the human eye reveals information that better reflects the actual visual experience.¹⁶ Hence, the complete experiment was repeated, this time simulating a polychromatic light source having three primary wavelengths (420, 589 and 760 nm) with equal weighting.

The resulting data pattern did not differ materially from that obtained with the monochromatic source. This result is in agreement with Jansonius and Kooijman,⁸ who found that chromatic aberrations minimally influenced relative modulation transfer functions. As the SCE relies on how the light interacts with the waveguide properties of the foveal cones, which is a process that is, in turn, completely wavelength-dependent,²⁴ the inclusion of SCE in the polychromatic model may not be appropriate and will not be discussed further.

DISCUSSION AND CONCLUSIONS

The impact of optical imperfections on the visual performance of the human eye has been of keen interest to vision scientists for most of the last century. While tremendous improvements have been made regarding the ability to objectively measure these defects, inadequate knowledge of their interaction with one another has generally limited the understanding of their visual effects. The obvious exception to this is defocus. For all kinds of refractive error, this is known to be the major ocular aberration and its effect on spatial visual performance metrics such as acuity and contrast sensitivity has been studied with great care. Visual performance as a function of defocus for an object having a given spatial frequency will be a reflection of the DoF that exists in the system. DoF becomes an important means of obtaining optimized vision in cases where significant defocus is evident as may occur, for example, at near vergences when accommodation is reduced (as in the case in presbyopic patients), or when it is entirely absent (for instance, after monofocal intraocular lens implantation).

The visual impact of changes in DoF can be assessed in a number of ways. It is well known that measuring contrast thresholds for sinusoidally modulated gratings for a range of spatial frequencies is an effective way of evaluating spatial vision.²⁵ Hence, contrast sensitivity functions over a range of defocus values are commonly used as a measure of the DoF.⁸ Alternatively, the DoF could also be defined as the range within which there is virtually no reduction in visual acuity.²⁶ Unfortunately, neither of these strategies is amenable to simulation using ray-tracing calculations. Therefore, it was necessary to take a different line in interpreting the results of

our modeling. Recalling that at a given spatial frequency the contrast sensitivity function is the product of the optical and the neural modulation transfer functions and knowing that defocus decreases the former but has no effect on the latter, we considered that the optical MTF should bear a direct linear relationship with the contrast sensitivity function. Since it is not feasible to incorporate neural factors into the ray tracing schema, we assumed these to be constant over all our models and selected the optical MTF as a predictor of visual performance. Hence the customary definition “peak width at half-maximum of MTF value” was considered as the adopted measure of DoF.

In the Zemax software, such MTF computations can be easily obtained by using the native settings of Fast-Fourier-Transform through-focus MTF (FFT MTF). This method slides the image surface, the retina in this case, moving it axially to produce the required amount of defocus. The MTF of the active configuration is then calculated for each point in the described range, while the spatial frequency in the image space is held constant. This is hardly physiological in the case of a real eye. Moreover, the dioptric differences that occurred due to the shifting of the focal plane in different directions could result in a slight asymmetry of the observed DoF measures. Additionally, spherical aberration could also be slightly affected by the displacement of the image position. Such factors complicate the findings obtained by the standard in-built methods. Hence, we have adopted the more robust through-focus MTF method, which consists of iterative paraxial lens corrections placed in front of the eye model.

In this experiment we have attempted to investigate the influence of the sign of the SA on the eye's DoF. Although the +SA and -SA results were close to being mirror images of one another for low-SF targets, there are some minor asymmetries in the DoF at higher SFs. Reviewing the DoF measures both from the through-focus MTF calculations as well as from the phase profile viewpoint, we noted that when SA was below (more negative than) $-0.15 \mu\text{m}$, the models showed marginally higher DoF than their positive-SA counterparts. An alternative explanation for this result could be given by considering the caustic envelope formed by the spherical aberration in any optical system. By definition, this envelope is different on either side of the best focus. The zone around the envelope's centre of least confusion is called the caustic core, and it is the portion that contributes to an increased depth-of-focus. This also switches from one side of focus to the other when the sign of spherical aberration is changed and lies closer to the exit pupil of the optical system with positive spherical aberration. As a result, there is a marginal increase in the numerical aperture of the system. Exactly the opposite happens in the negative-spherical-aberration case. Taking into account that image quality does not degrade as rapidly with defocus when numerical aperture is decreased, this fact might explain the slightly greater depth-of-focus found in the case of negative spherical aberration.

The results reinforce the theory that spherical aberration, be it positive or negative, increases the DoF. Moreover, certain higher levels of negative SA, either intrinsic or induced by means of external optical components, do occasionally result

in marginally higher levels of DoF than when the same magnitude of positive spherical aberration is present. This does not necessarily mean that image contrast will always be higher over a range of defocus. More importantly, such a small difference in DoF would not be sufficient to outweigh the effects of positive SA in mitigating presbyopic symptoms.

The explanation for the asymmetry in the through-focus MTF trends for positive and negative defocus might be well attributable to the strong Zernike-mode interaction between defocus and higher-order aberrations. This can probably be best comprehended by taking into account the geometrical optics of these two scenarios. In the positive SA model, when the retinal plane is shifted towards the hyperopic side, both SA and defocus add dioptrically and make the marginal rays to land farther away from the ideal location. On the other hand, when the retinal plane is moved towards the myopic side, the defocus now counterbalances the effect of SA, thereby improving the retinal image quality. The behavior of negative SA models and defocus could also be explained on a similar basis. This asymmetry around the optimum focus occurs particularly for mid and high spatial frequencies, i.e. around 10-30 cycles/mm, and for large pupil sizes, which is in good agreement with previous studies.²⁷⁻³⁰ In agreement with Zhang et al.,⁴ we also found that the SCE apodization has an impact on the quality of the defocused image only when defocus and spherical aberration have the same sign.

A key factor influencing the potential usefulness of these effects was pupil size. The DoF effects mentioned above were apparent in the initial modeling with a 6 mm pupil, which provided a wide range of SA, from -0.20 to +0.20 μm . However, with the 4 mm pupil, all the models showed more or less similar DoF values for every spatial frequency under study. The reason behind this result is that the smaller pupil size effectively eliminates from the calculations the SA associated with larger apertures. It is also important to recall that one of the operands of the merit function, as defined, is the emmetropic 2nd-order refraction taken over a 6 mm pupil. As the pupil size decreases, this non-zero refraction term brings down the central peak of the MTF. Understanding this point provides an insight into the design of aspheric multifocal contact and intraocular lenses, most of which have an optic diameter of about 6 to 8 mm. Thus, there is a wide zone in which the power can change, allowing control of SA across the whole optic of the lens. Light rays passing through the lens periphery can thus be utilized to promote the passive increase in DoF. Unfortunately, with the physiological pupil size usually varying between 3-5 mm, it is unlikely that this situation is achieved once the lens is in place on a real eye. Thus, it is likely that the actual DoF achieved would always be lower than the theoretical value.

The DoF was identical for both far and near vergences, a situation that can plausibly be attributed to the assumption that the aberration profiles of the unaccommodated and accommodated eyes were similar. This is certainly not the case among young adults, where SA is driven in the negative direction with accommodation, but it is closer to what happens among older people.³¹ The change of the aberration pattern with accommodation is strongly age-dependent and

is a complex function involving multiple variables. As this was not taken into account for the current isolated ray tracing experiment, comprehension of the effects of SA on DoF for a range of accommodative targets may be partial. This theoretical study is also arguably limited, as the subjective effects of viewing objects in the presence of spherical aberration have not been considered. Future work will be needed to remedy this.

We also considered whether the SCE, if exists, would contribute to a further increase in DoF. While theoretically this appeared to be the case, smaller pupil sizes, such as the typical values observed (3-4 mm) during everyday viewing conditions, substantially eliminate any effect. Moreover, the SCE was found to be beneficial only for the low-SF stimulus, with a mixed effect being evident for the mid and high SF's, commonly associated with reading and near tasks. In the light of this result, it is likely that the SCE will not usefully increase DoF in practical presbyopic correction situations.

As pointed out by Vohnsen,³² the pupil apodization technique used to model the SCE is subject to the aberration effects from the optics between the pupil plane and the retina. Unfortunately, due to the limitations of our modeling software we were not able to include such effects. As the aberrations incorporated into the present model appear to be less than those considered problematic by Vohnsen and, moreover, all previous experiments had been conducted using SCE neutralizing filters mounted in the pupil plane of the eye,^{22,27-30,33} we considered this approach to be reasonable. Nonetheless, readers should be aware, that the impact of the SCE on DoF in the presence of higher magnitudes of spherical aberration may differ slightly from those indicated here.

When it comes to considering the presbyopic-correction philosophy of using deliberately induced aberrations to increase the depth of focus, the current study indicates that certain amounts of positive or negative SA could have equal potential. However, for mid-to-high spatial-frequency tasks, which are typical of near and reading work, the experiment suggests that negative spherical aberration might be the preferred choice, although this will not result in all cases in higher DoF values. It should also be borne in mind that the amount of SA required to alleviate presbyopic symptoms is a function of pupil diameter and that, for close viewing distances, any residual accommodation will alter the effective ocular aberrations. These factors mean that, in practice, it would be a complex task to produce the calculated levels of DoF, since the combined spherical aberration of the corrective device and the eye would effectively need to be the same as that designed for the distant target.

A final point to be considered is that while certain high levels of negative SA do marginally improve the image contrast with defocus and effectively increase DoF, this increase is not symmetric about the best focus but, instead, it is limited to the myopic (positive defocus) side and, moreover, it is to a great extent spatial-frequency dependent. Therefore, it is likely that while manipulation of negative SA to raise the DoF might be achievable in some circumstances, these may not be sufficiently accessible to provide a useful improvement in near work in practical applications.

REFERENCES

1. Artal P, Benito A, Tabernero J. The human eye is an example of robust optical design. *J Vis.* 2006;6:1-7.
2. He JC, Marcos S, Burns SA. Comparison of cone directionality determined by psychophysical and reflectometric techniques. *J Opt Soc Am A Opt Image Sci Vis.* 1999;16:2363-2369.
3. Wang B, Ciuffreda KJ. Depth-of-focus of the human eye: theory and clinical implications. *Surv Ophthalmol.* 2006;51:75-85.
4. Zhang X, Ye M, Bradley A, Thibos L. Apodization by the Stiles-Crawford effect moderates the visual impact of retinal image defocus. *J Opt Soc Am A Opt Image Sci Vis.* 1999;16:812-820.
5. Nio YK, Jansonius NM, Fidler V, Geraghty E, Norrby S, Koosijman AC. Spherical and irregular aberrations are important for the optimal performance of the human eye. *Ophthalmic Physiol Opt.* 2002;22:103-112.
6. Charman WN. The Charles F. Prentice Award Lecture 2005: optics of the human eye: progress and problems. *Optom Vis Sci.* 2006;83:335-345.
7. McLellan JS, Marcos S, Prieto PM, Burns SA. Imperfect optics may be the eye's defence against chromatic blur. *Nature.* 9 2002;417:174-176.
8. Jansonius NM, Koosijman AC. The effect of defocus on edge contrast sensitivity. *Ophthalmic Physiol Opt.* 1997;17:128-132.
9. Vasudevan B, Ciuffreda KJ, Wang B. An objective technique to measure the depth-of-focus in free space. *Graefes Arch Clin Exp Ophthalmol.* 2006;244:930-937.
10. Marcos S, Moreno E, Navarro R. The depth-of-field of the human eye from objective and subjective measurements. *Vision Res.* 1999;39:2039-2049.
11. Charman WN, Jennings JA. The optical quality of the monochromatic retinal image as a function of focus. *Br J Physiol Opt.* 1976;31:119-134.
12. Holladay JT, Piers PA, Koranyi G, van der Mooren M, Norrby NE. A new intraocular lens design to reduce spherical aberration of pseudophakic eyes. *J Refract Surg.* 2002;18:683-691.
13. Jansonius NM, Koosijman AC. The effect of spherical and other aberrations upon the modulation transfer of the defocussed human eye. *Ophthalmic Physiol Opt.* 1998;18:504-513.
14. Khan S, Rocha G. Cataract surgery and optimal spherical aberration: as simple as you think? *Can J Ophthalmol.* 2008;43:693-701.
15. Piers PA, Fernandez EJ, Manzanera S, Norrby S, Artal P. Adaptive optics simulation of intraocular lenses with modified spherical aberration. *Invest Ophthalmol Vis Sci.* 2004;45:4601-4610.
16. Piers PA, Weeber HA, Artal P, Norrby S. Theoretical comparison of aberration-correcting customized and aspheric intraocular lenses. *J Refract Surg.* 2007;23:374-384.
17. Rocha KM, Soriano ES, Chamon W, Chalita MR, Nose W. Spherical aberration and depth of focus in eyes implanted with aspheric and spherical intraocular lenses: a prospective randomized study. *Ophthalmology.* 2007;114:2050-2054.
18. Somani S, Yee K. Presbyopia correction through negative high-order spherical aberration. U.S. Patent no 7261412 B2. 2007.
19. Bakaraju RC, Ehrmann K, Pappas E, Ho A. Finite schematic eye models and their accuracy to in-vivo data. *Vision Res.* 2008;48:1681-1694.
20. Escudero-Sanz J, Navarro R. Off-axis aberrations of a wide-angle schematic eye model. *J Opt Soc Am A Opt Image Sci Vis.* 1999;16:1881-1891.
21. Salmon TO, van de Pol C. Normal-eye Zernike coefficients and root-mean-square wavefront errors. *J Cataract Refract Surg.* 2006;32:2064-2074.
22. Applegate RA, Lakshminarayanan V. Parametric representation of Stiles-Crawford functions: normal variation of peak location and directionality. *J Opt Soc Am A.* 1993;10:1611-1623.
23. Goodman JW. Introduction to Fourier optics. New York: McGraw Hill, 1996.
24. Vohnsen B, Iglesias I, Artal P. Guided light and diffraction model of human-eye photoreceptors. *J Opt Soc Am A Opt Image Sci Vis.* 2005;22:2318-2328.
25. Campbell FW, Green DG. Optical and retinal factors affecting visual resolution. *J Physiol.* 1965;181:576-593.
26. Gupta N, Wolffsohn JS, Naroo SA. Optimizing measurement of subjective amplitude of accommodation with defocus curves. *J Cataract Refract Surg.* 2008;34:1329-1338.
27. Atchison DA, Joblin A, Smith G. Influence of Stiles-Crawford effect apodization on spatial visual performance. *J Opt Soc Am A Opt Image Sci Vis.* 1998;15:2545-2551.
28. Atchison DA, Marcos S, Scott DH. The influence of the Stiles-Crawford peak location on visual performance. *Vision Res.* 2003;43:659-668.
29. Atchison DA, Scott DH. Contrast sensitivity and the Stiles-Crawford effect. *Vision Res.* 2002;42:1559-1569.
30. Atchison DA, Scott DH, Strang NC, Artal P. Influence of Stiles-Crawford apodization on visual acuity. *J Opt Soc Am A Opt Image Sci Vis.* 2002;19:1073-1083.
31. Radhakrishnan H, Charman WN. Age-related changes in ocular aberrations with accommodation. *J Vis.* 2007;7:11 11-21.
32. Vohnsen B. Photoreceptor waveguides and effective retinal image quality. *J Opt Soc Am A Opt Image Sci Vis.* 2007;24:597-607.
33. Atchison DA, Woods RL, Bradley A. Predicting the effects of optical defocus on human contrast sensitivity. *J Opt Soc Am A Opt Image Sci Vis.* 1998;15:2536-2544.